Role of the tangential electric field component to the terahertz jet and hook formation by dielectric cube and sphere

Igor O. Dorofeev,*, Valentin I. Suslyaev, Oleg V. Minin, and Igor V. Minin
National Research Tomsk State University, Tomsk, Russia

Abstract. The mechanism of formation of a terahertz jet by a dielectric cuboid and a sphere surrounded by ideally conducting screens is considered. The maximum screen influence is observed when the screen is located near the alight cuboid base. The screen influence eases when the screen is shifting along the dielectric object. Power flux density localization area is almost completely shifted inside the object when the screen is situated in the center. The minimum influence is observed when screen placed in the shadow plane of the cuboid base. This effect caused by the screen influence on electric field component tangential to the side edges and thus on the power flux directed to the central axis of the object. The screen influence on the terahertz jet in spherical object has been compared. Value of the power flux density after passing the object is higher in a cuboid, but the focusing characteristics are better (appearing on shorter distances) in a sphere. © *2020 Society of Photo-Optical Instrumentation Engineers (SPIE)* [DOI: 10.1117/1.OE.60.8.082004]

Keywords: photonic jet; photonic hook; cuboid; metal screen; near-field microscopy.

Paper 20200778SS received Jul. 14, 2020; accepted for publication Sep. 10, 2020; published online Oct. 22, 2020.

1 Introduction

The problem of application of dielectric particles for lenses has long history. Presumably, such particles were first used in Antony van Leeuwenhoek's microscope on the eve of 1668.[1] In that case, a spherical particle was clamped in a special metal holder. Fundamentally, similar design is still used in the so-called nanoscopes based on spherical particles,[2–5] implementing the effect of the so-called photonic jet (PJ). However, no in-depth studies of the influence of the metal holder on the capability of a dielectric mesosize particle to form a local area of the electromagnetic field have been performed.

To date, many works have been published on the PJ effect. The authors of these works assert that the formation of areas of electromagnetic field concentration with size less than the classical diffraction limit is inherent in dielectric objects of different shapes and their sets.[6–9]

The localization areas parameters and the possibility of their control were studied both for homogeneous particles and for particles with a refractive index gradient as well as a multilayer structure.[10,11]

In addition to a consideration of isolated particles, cases when the PJ was formed in the presence of other objects have also been investigated. Microspheres with concentric conductive rings were studied in Ref. 12. In Ref. 13, the particle forming PJ represented the open end of the waveguide formed by plane-parallel metal guides. In Ref. 14, a spheroid was built in an optical fiber. In Ref. 15, a metal screen was used to screen partly the plane of a dielectric cuboid (parallelepiped) irradiated by an incident wave that led to anomalous apodization effect. Two dielectric bodies were investigated in Ref. 16. The focusing properties of dielectric particles in the reflection mode were investigated in Refs. 17–19 in the presence of a metallic screen and in Ref. 20 in the presence of a dielectric screen. The solution of these problems made it possible to establish new effects in those areas where focusing of the electromagnetic beam is important.[21–23]

*Address all correspondence to Igor O. Dorofeev, idorofeev@mail.tsu.ru

0091-3286/2020/$28.00 © 2020 SPIE

The practical application of the PJ effect involves the embedding of particles into a certain structure or waveguide path, as, for example, in Refs. 13 and 14. Typically, paths for optical and terahertz radiation are open or fiber optic (dielectric) channels. At the same time, for microwaves, the waveguide systems are mainly metal. Also, dielectric particles built in resonant metal structures can be used.[24–26] In all cases, it is necessary to study the effect of metal shields tightly covering a dielectric object on the features of PJ formation and its basic properties.

This work is aimed at elucidation of PJ formation mechanisms in the presence of a metal screen whose plane is parallel to the incident wave front and encompasses the dielectric object without gaps. The PJ formation by this object without screen was studied in a number of works (for example, see Ref. 27). This problem is important, for example, for systems of radiation input in and output from an open resonator. In this work, modeling was performed using the commercial software product CST Studio©. Taking into account the weak frequency dependence of the properties of metallic and most dielectric structures in the examined spectral range, the electric object sizes can be chosen fairly arbitrarily, so the problem can be scaled to the required optical, gigahertz, or terahertz frequencies.

2 Methodology

When the particle shaped as a cuboid is considered, it is suggested that the screen can be moved along the large side of the cuboid. Modeling of the plane wave incident on the dielectric cuboid surrounded by a metal perfectly conductive screen showed that its influence on the electromagnetic localization area in the near field (PJ) depends significantly on the mutual position of the screen and the dielectric object. Areas of strong influence of the screen leading to destruction of the field localization effect outside of the object are observed together with areas of practical absence of the screen influence on the PJ (or terahertz jet here) formation.

The incidence of the plane wave with frequency of 100 GHz ($\lambda_0 = 3$ mm) on a dielectric cuboid surrounded by a metal screen (Fig. 1) was considered. Calculations were performed with the following scaling parameters.

The cuboid base sides were $a = 3$ mm (λ_0, their coordinates were $-a/2 \le x \le a/2$ and $-a/2 \le y \le a/2$), and the larger side was 3.6 mm ($1.2\lambda_0$, coordinate $0 \le z \le$ b). The wave was incident from positive direction of the z axis, and the electric field vector was directed along the y axis. The relative dielectric permittivity of the material was $\varepsilon'/\varepsilon_0 = 2.13$, and the losses were absent: $\varepsilon''/\varepsilon_0 = 0$. The perfectly conductive screen was a square with side of 20 mm. These values were sufficient in order that to neglect the influence of diffraction on its edges. The screen thickness was $d = 0.2$ mm ($\lambda_0/15$).

As the key parameters characterizing the PJ, the full widths at half maximum (FWHM), that is, the widths of the jet at a level of half maximum of the jet power density in the corresponding z planes in the directions of the electric field polarization (y) and orthogonal to it (x) were used. The cubic particle (cuboid) formed almost circular localization area with FWHMx = FWHM$y = 0.44\lambda_0$ for the above-indicated parameters.[26]

Results of calculations of the FWHM parameters are given in Table 1 for the screen moving along the object ($L = b - d$, $L = b/2 - d/2$, and $L = 0$) and displaced by half the wavelength beyond the object limits with the rectangular aperture equal to the cuboid base area ($L = -\lambda_0/4$ and $L = -\lambda_0/2$) remaining unchanged.

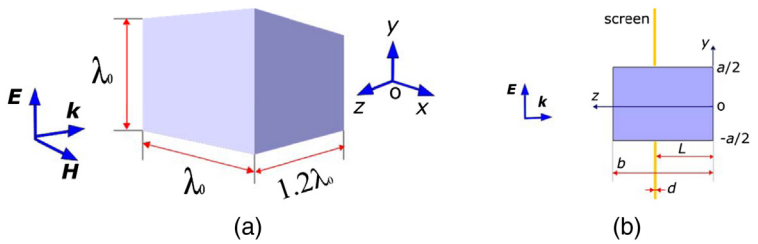

Fig. 1 (a) Incidence of the plane wave on the dielectric cuboid and (b) the screen placed at the distance L from the rare wall.

Table 1 FWHM in the $z = 0$ plane for different screen locations.

	Screen location, L	w/o screen	$L = b - d$	$L = b/2 - d/2$	$L = 0$	$L = -\lambda_0/4$	$L = -\lambda_0/2$
$z = 0$	FWHMx	$0.44\lambda_0$	$>\lambda_0$	$0.56\lambda_0$	$0.43\lambda_0$	$0.44\lambda_0$	$0.41\lambda_0$
	FWHMy	$0.44\lambda_0$	$>\lambda_0$	$0.51\lambda_0$	$0.43\lambda_0$	$0.43\lambda_0$	$0.45\lambda_0$

As shown in Table 1, the strongest influence of the screen is observed when it is located at the cuboid base nearest to the incident wave. As the screen moves toward the far dielectric object base, its influence weakens and reaches a minimum when the screen is in the plane of the far cuboid base. This result confirms the fact that the localization area is formed by the lateral cuboid sides,[28] unlike the spherical particle where the PJ formation is caused by refraction.

From the results presented above, we can conclude that inside the object areas with electric field component tangential to the upper and lower sides [E_z, Fig. 2(a)] can be observed. The field amplitude in these areas increases in the direction of wave propagation. It is also in phase with the magnetic field component [H_x, Fig. 2(b)] in these areas. As a result, the component of the power flow [$P_y \sim E_z H_x$, Fig. 2(c)] directed toward the z axis (in the negative direction of the y axis in the upper half of the object where it is depicted by dark blue color and in the positive direction in the lower half of the object where it is depicted by red color) that leads to the localization of power flow density along the wave propagation direction [P_z, Fig. 2(d)] and moving the area outside the object. Since all models are constructed for a plane incident wave directed toward the negative values of the z axis, the P_z component at its maximum will have a minus sign (depicted by dark blue color).

In the presence of a perfectly conducting screen, the field component at the place of its contact with the dielectric disappears, and a reflected wave appears. The example with the screen placed in the cuboid center is shown in Fig. 3. As a result of reflection, the amplitude of the tangential electric field component increases in the direction opposite to that of wave propagation and weakens in the direction of wave propagation [Fig. 3(a)].

At the same time, the distribution of the magnetic field component H_x [Fig. 3(b)] also changes, which leads to the formation of the power flow density components directed toward the z axis in front of the screen [P_y, Fig. 3(c)] and to the displacement of the power flow density concentration area in the direction of wave propagation inside the object [P_z, Fig. 3(d)].

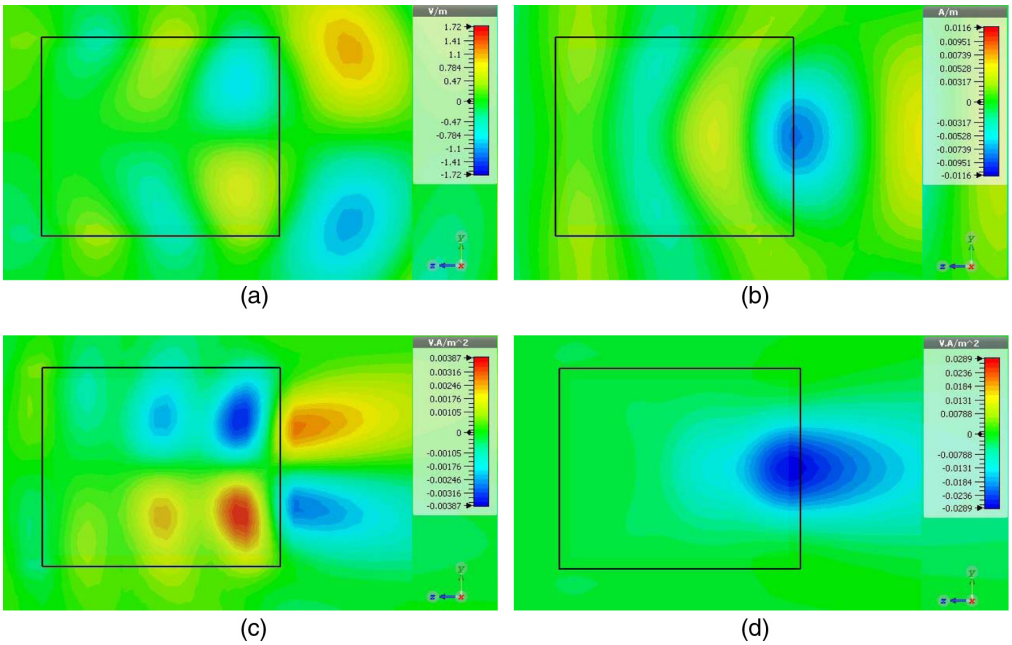

(a) (b)

(c) (d)

Fig. 2 Distribution of the field components: (a) E_z and (b) H_x, and components of the power flow density vector (c) P_y, and (d) P_z in the plane $x = 0$. The screen is absent.

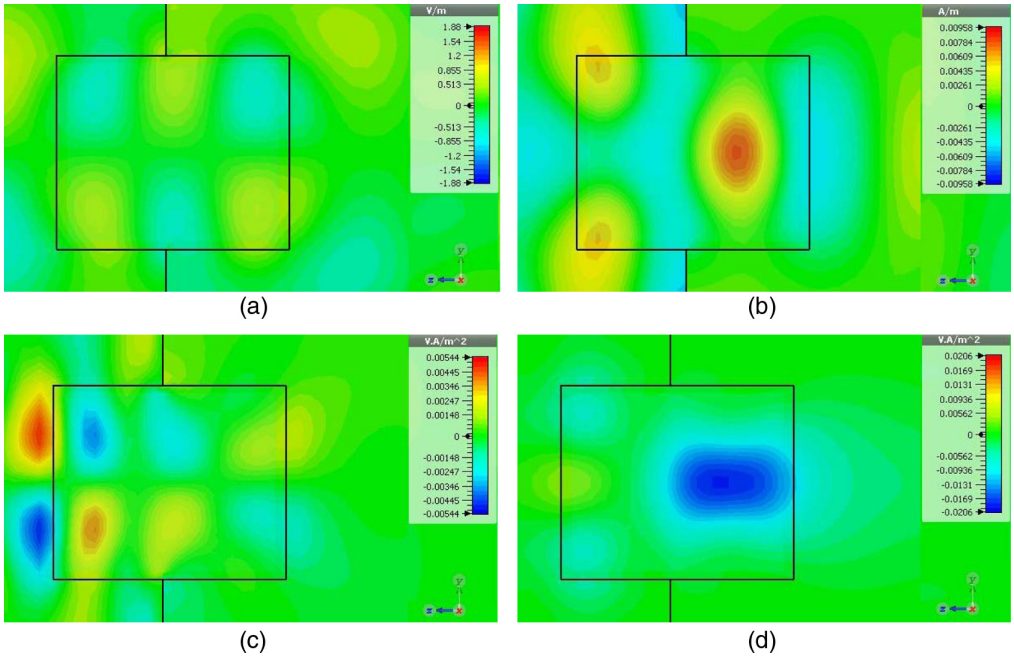

Fig. 3 Distribution the field components: (a) E_z and (b) H_x, and components of the power flow density vector (c) P_y and (d) P_z in the plane $x = 0$. The screen is located in the cuboid center ($L = b/2 - d/2$).

Table 2 gives results of calculations in the planes at distances $z = -0.1\lambda_0$ and $z = -0.2\lambda_0$ from the shadowed cuboid side when the screen is placed outside of the object.

In these cases, the screen influences insignificantly on the fields inside of the object, and the PJ is formed approximately in the same conditions as without the screen. Only a small deformation (broadening) of the field localization areas within the limits of 10% of FWHM change is observed. When the screen is placed at a distance of half the wavelength, a small decrease of the cross sectional PJ area is observed at the distance $0.2\lambda_0$ from the dielectric plane in comparison with the screen absence (the effect of stretching of the area for which FWHM $< \lambda_0/2$).

As a whole, modeling has also shown that the processes of PJ formation in the direction orthogonal to the electric field polarization direction occur analogously.

Also, the comparison of the results obtained with a shield around a dielectric sphere is interesting. Figure 4 shows the distribution of the component of the electric field (E_z), magnetic field (H_x), and of the components of the power flow density vector (P_y, P_z).

As in the case with the cuboid, the presence of the screen leads to the formation of the reflected wave and redistribution of the longitudinal electric field component (E_z) (decrease of the maxima in the direction of wave propagation) as well as to the change of the distribution of the magnetic field component (H_x). Because of this, the maxima of the components of the power flow density vector, which forms jet in the direction of wave propagation are displaced toward the screen, and the concentration area shifts into the object.

In addition, in the presence of a screen inside the particle [Fig. 4(c)], two maxima of the power flux density appear (yellow at the top and blue at the bottom), which lead to the

Table 2 FWHM in planes $z = -0.1\lambda_0$ and $z = -0.2\lambda_0$ for different screen locations.

	Screen location, L	w/o screen	$L = 0$	$L = -\lambda_0/4$	$L = -\lambda_0/2$
$z = -0.1\lambda_0$	FWHMx	$0.44\lambda_0$	$0.48\lambda_0$	$0.48\lambda_0$	$0.44\lambda_0$
	FWHMy	$0.46\lambda_0$	$0.45\lambda_0$	$0.44\lambda_0$	$0.46\lambda_0$
$z = -0.2\lambda_0$	FWHMx	$0.51\lambda_0$	$0.52\lambda_0$	$0.49\lambda_0$	$0.47\lambda_0$
	FWHMy	$0.51\lambda_0$	$0.48\lambda_0$	$0.50\lambda_0$	$0.47\lambda_0$

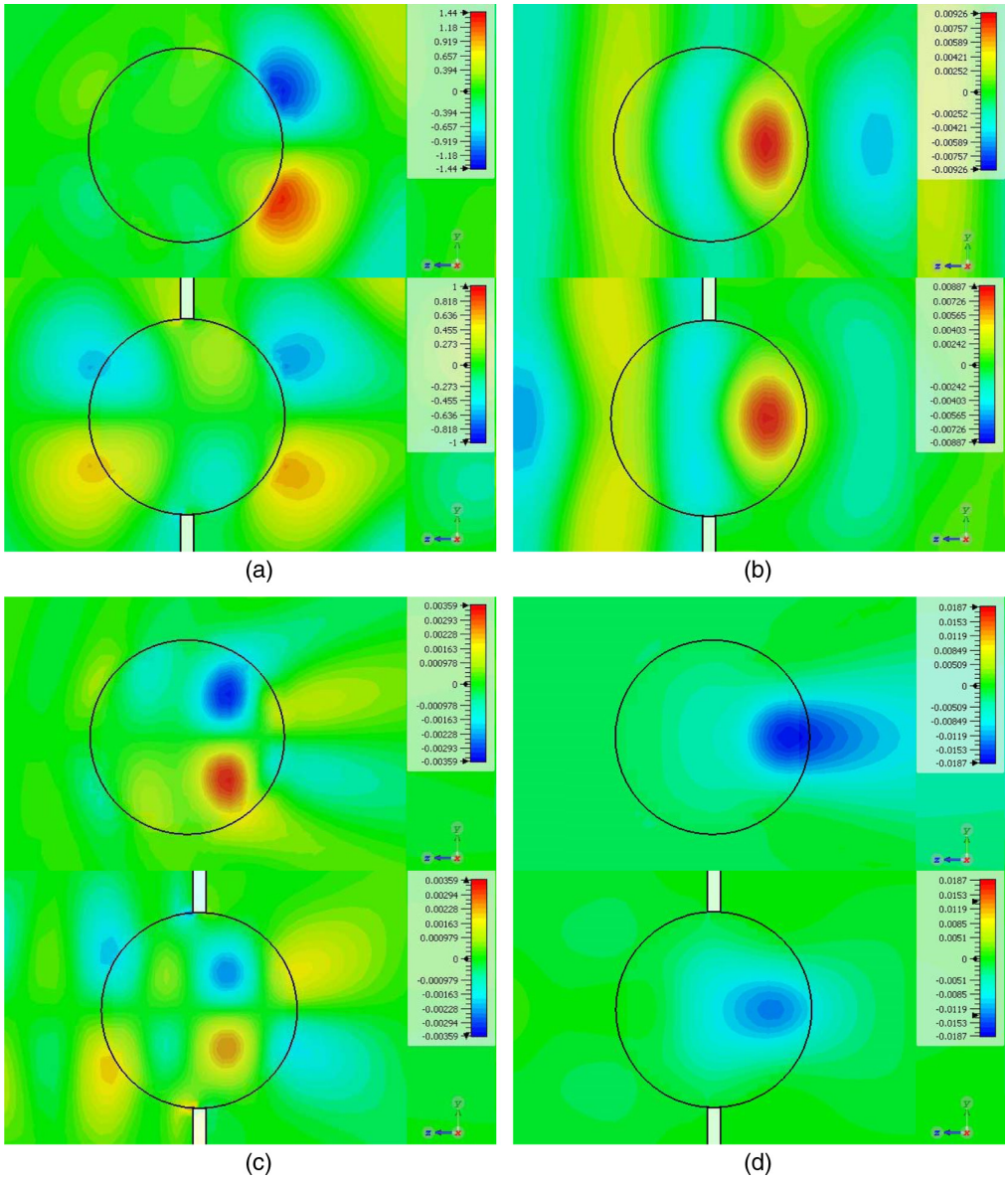

Fig. 4 Distribution the field components: (a) E_z and (b) H_x, and the components of the power flow density vector: (c) P_y and (d) P_z in the plane $x = 0$.

divergence of the wave. For a free particle, the direction of the power flux inside it (P_y) is such that focusing occurs.[27,28]

Here, unlike the cuboid, focusing is observed at smaller distances due to the surface curvature of the sphere.

Figure 5 shows the plots of the power flow density distribution in the shadowed plane ($z = 0$).

The results obtained indicate that in the presence of a screen, the power flux density after passing the object is higher for a cuboid; at the same time, the focusing properties of the sphere are better.

Let us briefly consider two main applications of these effects. The case in which the cuboid length was halved was also considered; in this case, the screen located in the center of the object was displaced toward its shadowed plane. Here, the field localization area was outside of the object (Fig. 6).

The calculated values of its parameters were FWHMx $= 0.47\lambda_0$ and FWHMy $= 0.49\lambda_0$. Thus, the given object allows the PJ to be formed; moreover, the PJ sizes were also halved

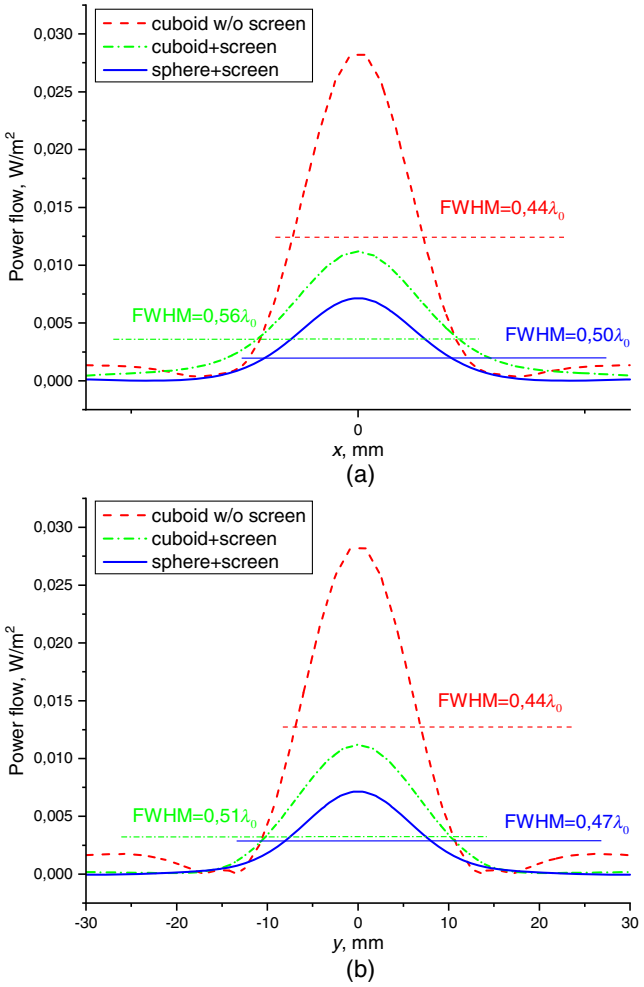

Fig. 5 Distribution of the power flow density P_z in (a) the shadowed plane ($z = 0$) in the orthogonal direction and (b) in the direction of the electric field vector polarization for the sphere and the cuboid surrounded by the screen in comparison with the distributions for the cuboid without screen.

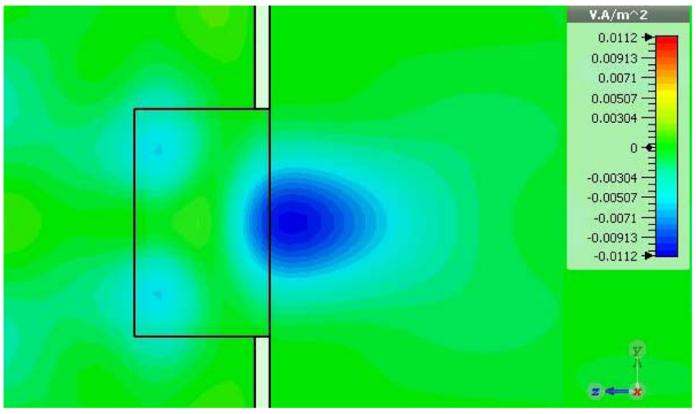

Fig. 6 Area of localization of the power flow density for the cuboid whose size was halved with preservation of the metal screen.

compared to those for the initial cuboid. The power flow density in the localization area was much less than for the full-size object without screen due to the occurrence of the reflected wave.

Another interesting possibility of controlling the form of radiation localization is the asymmetric control of the tangential component of the energy flux inside the cube. In this regard, we

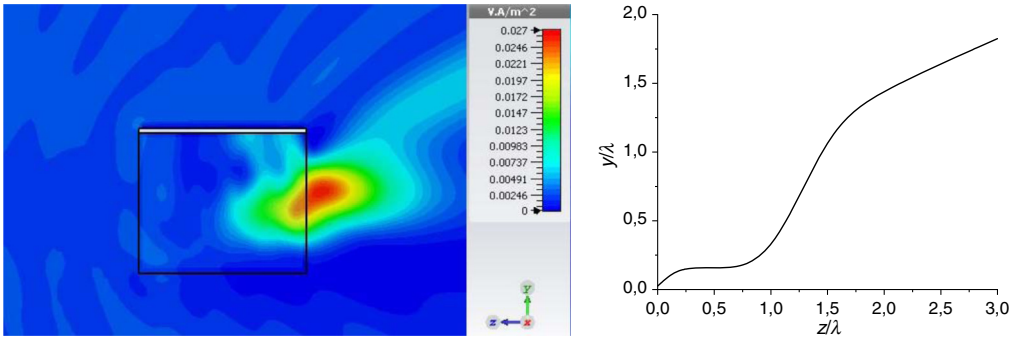

(a) (b)

Fig. 7 (a) Power flux density distribution in the $x = 0$ plane. (b) Displacement from the axis $0Z$ of the maximum power flux density depending on the distance to the shadow surface of the cuboid.

can talk about a new method of forming the so-called photonic hook.[28–31] Since in this example, shown in Fig. 7, the metal screen completely covers only the upper face of the cubic particle, the power flow shifts toward the upper face. Moreover, for the accepted particle parameters and screen sizes, the minimum value of the beam width is about FWHM $\sim 0.6\lambda$. As a result, the region of the field localization outside the particle is curved, which opens up the possibility of the formation of specified configurations of localized fields. But this is the task of future research.

3 Conclusion

Thus, the dielectric particles shaped as a cuboid forming the PJ can be built in metal screens by placing these screens in the plane of the object furthest in the direction of wave incidence or behind this plane. For the sphere, the presence of the metal screen tangential to its surface in the central cross section will displace the power flow density localization area inside of this sphere, which demonstrates impossibility of embedding of spherical particles into microwave metal structures with retention of the PJ outside of the object.

The cuboid with the screen located in its shadowed side whose length is half that of the initial object without screen can also be used to obtain the power flow density localization area with aperture smaller than $\lambda_0/2$. Control the tangential electric field component by metal screen allows to deflect the PJ.

Results of this work can be used to design objects forming electromagnetic field localization area of the PJ type in the directing, reflecting, bending, and resonant elements of optical type in such devices, as systems of near-field microscopy (local diagnostics of materials and objects), sensors, etc.

Acknowledgments

This research was supported by Ministry of Science and Higher Education of the Russian Federation, project No. 0721-2020-0038, and was partially supported by the Russian Foundation for Basic Research (Grant No. 20-57-S52001).

References

1. C. Dobell, *Antony van Leeuwenhoek and His "Little Animals,"* Harcourt, Brace and Company, New York (1932).
2. A. Jacassi et al., "Scanning probe photonic nanojet lithography," *ACS Appl. Mater. Interfaces* **9**(37), 32386–32393 (2017).
3. M. Duocastella et al., "Combination of scanning probe technology with photonic nanojets," *Sci. Rep.* **7**, 3474 (2017).

4. J. J. Wang, D. McCloskey, and J. F. Donegan, "Optimization of parameters of photonic nanojet generated by dielectric microsphere for laser nanojet SNOM," *Proc. SPIE* **8321**, 83213Z (2011).
5. L. A. Krivitsky et al., "Locomotion of microspheres for super-resolution imaging," *Sci. Rep.* **3**(1), 3501 (2013).
6. B. S. Luk'yanchuk et al., "Refractive index less than two: photonic nanojets yesterday, today and tomorrow [Invited]," *Opt. Mater. Express* **7**(6), 1820 (2017).
7. I. V. Minin, O. V. Minin, and Y. E. Geints, "Localized EM and photonic jets from non-spherical and non-symmetrical dielectric mesoscale objects: brief review," *Ann. Phys.* **527**(7–8), 491–497 (2015).
8. C.-Y. Liu and F.-C. Lin, "Geometric effect on photonic nanojet generated by dielectric microcylinders with non-cylindrical cross-sections," *Opt. Commun.* **380**, 287–296 (2016).
9. C.-Y. Liu, O. V. Minin, and I. V. Minin, "Periodical focusing mode achieved through a chain of mesoscale dielectric particles with a refractive index near unity," *Opt. Commun.* **434**, 110–117 (2019).
10. C.-Y. Liu, "Superenhanced photonic nanojet by core-shell microcylinders," *Phys. Lett. A* **376**(23), 1856–1860 (2012).
11. C.-Y. Liu et al., "Engineering photonic nanojet by a graded-index micro-cuboid," *Physica E* **98**, 105–110 (2018).
12. M. X. Wu et al., "Modulation of photonic nanojets generated by microspheres decorated with concentric rings," *Opt. Express* **23**(15), 20096–20103 (2015).
13. B. Ounnas et al., "Single and dual photonic jets and corresponding backscattering enhancement with tipped waveguides: direct observation at microwave frequencies," *IEEE Trans. Antennas Propag.* **63**(12), 5612–5618 (2015).
14. L. Han et al., "Controllable and enhanced photonic jet generated by fiber combined with spheroid," *Opt. Lett.* **39**(6), 1585 (2014).
15. L. Yue et al., "Millimetre-wave cuboid solid immersion lens with intensity-enhanced amplitude mask apodization," *J. Infrared Millimeter Terahertz Waves* **39**(6), 546–552 (2018).
16. J. Yang et al., "Ultra-narrow photonic nanojets through a glass cuboid embedded in a dielectric cylinder," *Opt. Express* **26**(4), 3723 (2018).
17. I. V. Minin, O. V. Minin, and N. A. Kharitoshin, "Localized high field enhancements from hemispherical 3D mesoscale dielectric particles in the refection mode," in *16th Int. Conf. Young Specialists Micro/Nanotechnol. and Electron Devices*, IEEE, pp. 331–333 (2015).
18. I. V. Minin et al., "Localized photonic jets from flat, three-dimensional dielectric cuboids in the reflection mode," *Opt. Lett.* **40**(10), 2329 (2015).
19. I. V. Minin et al., "Experimental observation of flat focusing mirror based on photonic jet effect," *Sci. Rep.* **10**, 8459 (2020).
20. L. Yue et al., "Photonic jet by a near-unity-refractive-index sphere on a dielectric substrate with high index contrast," *Ann. Phys.* **530**, 1800032 (2018).
21. B. Born et al., "Integration of photonic nanojets and semiconductor nanoparticles for enhanced all-optical switching," *Nat. Commun.* **6**(1), 8097 (2015).
22. M. P. L. Sentis, F. R. A. Onofri, and F. Lamadie, "Bubbles, drops, and solid particles recognition from real or virtual photonic jets reconstructed by digital in-line holography," *Opt. Lett.* **43**(12), 2945 (2018).
23. O. V. Minin, I. V. Minin, and N. Kharitoshin, "Microcubes aided photonic jet scalpel tips for potential use in ultraprecise laser surgery," in *Int. Conf. Biomed. Eng. and Comput. Technol.*, IEEE, pp. 18–21 (2015).
24. I. O. Dorofeev et al., "Small-sized body influence on the quality factor increasing of quasioptical open resonator," *Opt. Quantum Electron.* **49**, 355 (2017).
25. V. I. Suslyaev et al., "An investigation of electromagnetic response of composite polymer materials containing carbon nanostructures within the range of frequencies 10 MHz-1.1 THz," *Russ. Phys. J.* **55**(8), 970–976 (2013).
26. I. O. Dorofeev and G. E. Dunaevskii, "Resonance characteristics for microwire pieces as elements of composite materials," *Russ. Phys. J.* **59**(12), 2080–2086 (2017).

27. V. Pacheco-Peña et al., "Terajets produced by dielectric cuboids," *Appl. Phys. Lett.* **105**(8), 084102 (2014).
28. I. V. Minin and O. V. Minin, *Diffractive Optics and Nanophotonics: Resolution Beyond the Diffraction Limit*, Springer, Cham (2016).
29. I. V. Minin et al., "Experimental observation of a photonic hook," *Appl. Phys. Lett.* **114**(3), 031105 (2019).
30. O. V. Minin et al., "Electromagnetic field localization behind a mesoscale dielectric particle with a broken symmetry: a photonic hook phenomenon," *Proc. SPIE* **11368**, 1136807 (2020).
31. I. V. Minin et al., "Recent advantages in integrated photonic jet-based photonics," *Photonics* **7**(2), 41 (2020).

Biographies of the authors are not available.